*J. Fluid Mech.* (1991), *vol.* 226, *pp.* 573–590
*Printed in Great Britain*



# Asymptotic evaluation of three-dimensional wave packets in parallel flows

By FENG JIANG
Cambridge University Engineering Department, Trumpington Street, Cambridge CB2 1PZ, UK

(Received 19 December 1989)

This paper examines the three-dimensional wave packets which are generated by an initially localized pulse disturbance in an incompressible parallel flow and described by a double Fourier integral in the wavenumber space. It aims to clear up some confusion arising from the asymptotic evaluation of this integral by the method of steepest descent. In this asymptotic analysis, the calculation of the eigenvalues can be facilitated by making use of the Squire transformation. It is demonstrated that the use of the Squire transformation introduces branch points in the saddle-point equation that links the physical coordinates to the saddle-point value, regardless of whether the flow is viscous or inviscid. It is shown that the correct branch should be chosen according to the principle of analytic continuation. The saddle-point values for the three-dimensional problem should be considered to be the analytic continuation of those for the two-dimensional case where the saddle-point values can be uniquely determined. The three-dimensional wave packets in an inviscid wake flow are examined; their behaviour at large time is calculated asymptotically by the method of steepest descent in terms of the two-dimensional eigenvalue relation.

## 1. Introduction

Laminar flows break down into turbulence owing to the growth of wavy disturbances excited by external sources. The classic linear stability theory analyses eigenmodes in a flow system, and determines whether the flow is stable or unstable for some particular modes (e.g. Lin 1955; Betchov & Criminale 1967; Drazin & Reid 1981). However, it is currently known that it is more relevant to model laminar–turbulence transitions in real flows by studying the evolution of wave packets generated by isolated pulse disturbances (see, for example, Benjamin 1961; Criminale & Kovasznay 1962; Betchov & Szewczyk 1963; Gaster & Davey 1968; Gaster & Grant 1975). This is because natural transition usually involves wave modes with a broad range of frequencies and wavelengths. When these modes develop in an unstable flow, they form wave packets, which in turn evolve into turbulent spots at the beginning of the transition process. A pulse-type disturbance has a flat spectrum, so that all possible modes can be excited by applying such a disturbance to a flow. Through selective amplification, those modes that are unstable grow with time. Close to transition, it is the rapid exponential growth of the unstable modes, rather than the detailed nature of the initial excitation, that is the dominant feature in the flow. Thus the wave packets generated by idealized pulse excitations can very satisfactorily model those occurring in natural situations which are produced by disturbances such as free-stream turbulence.

A wave packet generated by an initially localized disturbance in an incompressible parallel flow can be represented, in linear theory, by inverse Fourier transforms in

wavenumber space, containing contributions from both the continuous spectrum and from all the discrete eigenmodes. Because of the exponential growth in the linear region of their development, the unstable waves are increasingly dominated by the fastest growing mode as they evolve with time. The wave packet formed by this dominant mode can be calculated by making use of the method of steepest descent with the dominant contribution given by saddle points (Gaster 1968*a*). The determination of saddle points is accordingly a matter of calculating eigenvalues and their derivatives. It is well known that the eigenvalue relation for a three-dimensional problem, whether viscous or inviscid, can be connected to a corresponding two-dimensional one by the Squire transformation. This transformation significantly reduces the burden of calculation, as eigenvalues are only then required for a two-dimensional problem. However, it creates some difficulties that must be carefully dealt with, especially when it is used in the asymptotic analysis. Because the transformation involves squared functions, it renders the wavenumbers double-valued, and presents the problem of choosing the correct branch for them. This has caused some difficulties in Gaster & Davey's study (1968) of the asymptotic behaviour of the wave packet generated by a pulse disturbance in an inviscid wake flow. They found a spurious discontinuity which they conjectured might be the first region to break down into turbulence. As a corollary of this they suggested that inviscid theory might not be sufficient to model the real viscous flow in some cases. To clarify this, we will examine in detail the singularities introduced by using the Squire transformation. It will be shown that the difficulties Gaster & Davey encountered are entirely due to the branch cut introduced by the Squire transformation and are not related to any physical phenomena. They can all be overcome by establishing a criterion for the choice of the relevant branch according to the principle of analytic continuation. We will show that this criterion can be derived from the fact that the solution of the three-dimensional problem is the analytic continuation of the equivalent two-dimensional problem. Any choice of the branch in the asymptotic solution must ensure that the chosen branch contains the relevant two-dimensional solution. As an example, the parallel wake flow discussed by Gaster & Davey (1968) will be examined. For this wake flow the unstable waves are convective in nature; they propagate with their group velocity downstream in the mean flow direction with increasing amplitudes. The three-dimensional wave packet generated by a pulse excitation occupies an almost elliptic region with a slightly concave forward face.

## 2. Formulation of the problem

Consider an incompressible parallel flow that is perturbed by a small impulsive force activated from some initial instant. For the sake of convenience, we assume that all variables have been non-dimensionalized. The mean flow is assumed to be in the positive $x$-direction of a Cartesian coordinate system $(x, y, z)$, with a non-dimensional velocity profile $\bar{U}(y)$, and the external disturbance force to be applied to the flow system acts in the direction perpendicular to the mean flow. By linearizing the Navier–Stokes equation, a set of linear partial differential equations for the perturbation velocities $(\hat{u}, \hat{v}, \hat{w})$ and pressure $\hat{p}$ can be derived (Lin 1955). Eliminating $\hat{u}$, $\hat{w}$ and $\hat{p}$ from these equations, a single partial differential equation for $\hat{v}$ can be derived, whose coefficients are functions of $y$ only, which thus can be conveniently solved by using Fourier transforms. Since the localized forcing is switched on at some initial instant, $t = 0$ say, and the disturbances produced by the forcing propagate

through the flow at finite speeds, the disturbances can only travel a finite distance from the forcing point in any finite time period. Thus, the perturbation velocity $\hat{v}(x, y, z, t)$ is always zero for $|x| \to \infty$ and $|z| \to \infty$ at any finite time $t$. The Fourier transforms in the $x$- and $z$-directions then exist in the conventional sense, which means that, if $a$ and $b$ are the wavenumbers in the $x$- and $z$-directions respectively, the inverse transformations from the wavenumber space $(a, b)$ to the physical space $(x, z)$ are ordinary real variable transformations. To perform the Fourier transform with respect to time $t$, it is necessary to assign an imaginary part to the frequency parameter $\tilde{\omega}$ such that this imaginary part is larger than the faster growth rate of the disturbances, which offsets the growth of instability waves at large time and ensures the convergence of the Fourier transform from the time to the frequency domain. The use of Fourier transformations reduces the partial differential equation to an ordinary differential equation for $v(y, a, b, \tilde{\omega})$, which is to be solved subject to typical boundary conditions

$$v = \frac{\partial v}{\partial y} = 0 \quad \text{as} \quad y \to \pm\infty.$$

The solution $v$ can be found as the ratio of a function $F$ and the Wronskian $\Delta$ of the Orr–Sommerfeld equation calculated at $y = 0$, i.e.

$$v(y, a, b, \tilde{\omega}) = \frac{F(y, a, b, \tilde{\omega})}{\Delta(a, b, \tilde{\omega})}.$$

The definition of the function $F$ is omitted here since it is not of concern. Then the velocity $\hat{v}$ in the physical space $(x, y, z, t)$ is given by the inverse Fourier transform,

$$\hat{v}(x, y, z, t) = \frac{1}{(2\pi)^3} \int_a \int_b \int_{\tilde{\omega}} \frac{F(y, a, b, \tilde{\omega})}{\Delta(a, b, \tilde{\omega})} \exp\left[\mathrm{i}(ax + bz - \tilde{\omega}t)\right] \mathrm{d}\tilde{\omega}\, \mathrm{d}a\, \mathrm{d}b,$$

where the wavenumber integrals are along the real axes in the complex $a$- and $b$-planes and the frequency inversion is performed along a horizontal line from $-\infty$ to $+\infty$ in the complex $\tilde{\omega}$-plane above all the singularities of the integrand. The $\tilde{\omega}$-integral can be performed by making use of the residue theorem. For $t < 0$, the integration contour must be closed by a semi-circle in the upper half of the $\tilde{w}$-plane to allow the integral to converge. Since there are no singularities above the integration path, the solution for $t < 0$ is then identically zero, a result in accordance with the principle of causality. On the other hand, for $t > 0$, convergence requires the contour to be closed in the lower half of the $\tilde{\omega}$-plane so that contributions come from all the singularities (from the dispersion relation) and branch cuts. The former are usually poles and yield discrete modes while the latter correspond to continuous spectra.

## 3. The saddle-point method

For the long-term behaviour of the disturbance, however, the fastest component will be dominant and this comes from the discrete eigenmode with the largest imaginary part. Thus the asymptotic behaviour of the disturbance velocity $\hat{v}(x, y, z, t)$ is characterized by a double integral in the wavenumber space,

$$\hat{v}(x, y, z, t) = \frac{1}{(2\pi)^2 \mathrm{i}} \int_a \int_b g(a, b, y) \exp\left[\psi(a, b)\, t\right] \mathrm{d}a\, \mathrm{d}b, \tag{3.1}$$

where the complex phase function $\psi(a,b)$ is defined as

$$\psi = \mathrm{i}\left[a\frac{x}{t}+b\frac{z}{t}-\tilde{\omega}(a,b)\right], \tag{3.2}$$

and the integrand has been denoted by $g(a,b,y)$, that is,

$$g(a,b,y) = \frac{F(a,b,\tilde{\omega},y)}{\partial\Delta(a,b,\tilde{\omega})/\partial\tilde{\omega}},$$

with $\tilde{\omega}(a,b)$ the most unstable complex eigenfrequency determined by $\Delta(a,b,\tilde{\omega})=0$. As first advocated by Gaster (1968*a*), the method of steepest descent can be applied to non-conservative wave systems with complex eigenfrequency $\tilde{\omega}(a,b)$ such as that represented by (3.1). The dominant contributions to the double integral as $t\to\infty$, while $x/t$ and $z/t$ remain constant, are from the saddle points of $\psi$ and the singularities of $g(a,b,y)$. This results from deforming the original integration paths along the real axes onto the steepest descent paths in the complex $a$- and $b$-planes. In doing so, contributions from the relevant singularities of $g(a,b,y)$ must be collected and those from the steepest descent paths come predominantly from the saddle points. The pole contributions can be analysed by the residue theorem, which requires the determination of the eigenfunctions of the governing equation. For the asymptotic analysis with $t\to\infty$, we will concentrate on the saddle-point contribution.

For given $(x/t, z/t)$ and Reynolds number $\widetilde{Re}$, the saddle point is given by the vanishing of the gradient of the complex phase function $\psi(a,b)$, namely, $\partial\psi(a,b)/\partial a = 0$ and $\partial\psi(a,b)/\partial b = 0$. By making use of the definition (3.2), this leads to

$$\frac{\partial\tilde{\omega}(a,b)}{\partial a}=\frac{x}{t}, \quad \frac{\partial\tilde{\omega}(a,b)}{\partial b}=\frac{z}{t}. \tag{3.3}$$

Following Gaster (1968*a*), the leading-order contribution to the double integral (3.1) can be found as

$$\hat{v}(x,y,z,t) = -\frac{g(a,b,y)\exp\left[\psi(a,b)\,t\right]}{2\pi t[-J(a,b)]^{\frac{1}{2}}}, \tag{3.4}$$

provided that the Jacobian determinant of the second derivatives, defined by

$$J = \begin{vmatrix} \dfrac{\partial^2\psi}{\partial a^2} & \dfrac{\partial^2\psi}{\partial a\,\partial b} \\ \dfrac{\partial^2\psi}{\partial a\,\partial b} & \dfrac{\partial^2\psi}{\partial b^2} \end{vmatrix} = -\frac{\partial^2\tilde{\omega}}{\partial a^2}\frac{\partial^2\tilde{\omega}}{\partial b^2}+\left(\frac{\partial^2\tilde{\omega}}{\partial a\,\partial b}\right)^2, \tag{3.5}$$

does not vanish. All the quantities $a, b, \tilde{\omega}(a,b)$ and the derivatives of $\tilde{\omega}(a,b)$ in (3.4) and (3.5) take their values at the saddle point, determined by (3.3). In the case where the Jacobian determinant (3.5) does vanish, the leading-order term of the asymptotic expansion will be of order $1/t^{\gamma}$ with $\gamma<1$. The values of $\gamma$ depend on how many terms among $\partial^2\psi/\partial a^2$, $\partial^2\psi/\partial a\,\partial b$ and $\partial^2\psi/\partial b^2$ are zero.

The result (3.4) describes the development of wave packets. At any given point $(x/t, z/t)$ in the physical space, if the real part of the complex phase function $\psi$ is positive, the disturbances grow with time; otherwise the waves decay as they travel in the flow and the flow eventually returns to its undisturbed state. Note that keeping the pair $(x/t, z/t)$ constant corresponds to an observation position moving with constant velocity

$$\left\{\frac{x}{t}, \frac{z}{t}\right\} = \left\{\frac{\partial\tilde{\omega}}{\partial a}, \frac{\partial\tilde{\omega}}{\partial b}\right\},$$

where the last step follows from the use of (3.3). Thus the result (3.4) actually describes the waves in the frame of reference of an observer moving with the group velocity of the waves. This moving observer sees the waves growing or decaying according to whether the real part of $\psi$ is positive or negative. Of course, if the observation position is at a fixed point $(x, y, z)$, the characteristics of the waves depend on whether the flow is convectively or globally unstable.

The evaluation of the result (3.4) (or (3.1) by numerical summation) requires the values of the eigenfrequency $\tilde{\omega}(a, b)$ for the three-dimensional problem. The calculation of $\tilde{\omega}(a, b)$ for the given $\tilde{R}e$ can be greatly facilitated by making use of the Squire transformation,

$$\left.\begin{aligned} \alpha^2 &= a^2+b^2 \\ \alpha Re &= a\tilde{R}e \\ \frac{\omega}{\alpha} &= \frac{\tilde{\omega}}{a} \end{aligned}\right\}, \tag{3.6}$$

where $\alpha$, $\omega$ and $Re$ are respectively the wavenumber, frequency and Reynolds number in the corresponding two-dimensional problem. Thus the evaluation of $\tilde{\omega}(a, b)$ for the different $\tilde{R}e$ is reduced to the evaluation of $\omega(\alpha, Re)$, which is determined by the Orr–Sommerfeld equation.

## 4. Singular points introduced by the Squire transformation

To demonstrate that the Squire transformation introduces singularities, we will discuss the viscous problem in this section. By making use of the two-dimensional eigenfrequency $\omega(\alpha, Re)$, the saddle-point equations (3.3) can be converted through the transformation (3.6) to

$$\left.\begin{aligned} \frac{x}{t} &= \left(\frac{\partial\omega}{\partial\alpha}-\frac{\omega}{\alpha}-\frac{Re}{\alpha}\frac{\partial\omega}{\partial Re}\right)\frac{a^2}{\alpha^2}+\frac{\omega}{\alpha}+\frac{Re}{\alpha}\frac{\partial\omega}{\partial Re} \\ \frac{z}{t} &= \left(\frac{\partial\omega}{\partial\alpha}-\frac{\omega}{\alpha}-\frac{Re}{\alpha}\frac{\partial\omega}{\partial Re}\right)\frac{ab}{\alpha^2} \end{aligned}\right\}. \tag{4.1}$$

On eliminating $a$ and $b$ from these equations, a single equation relating the physical parameters $(x/t, z/t)$ to the two-dimensional wavenumber $\alpha$ can be formulated,

$$\left(\frac{x}{t}-\frac{\partial\omega}{\partial\alpha}\right)\left(\frac{x}{t}-\frac{\omega}{\alpha}-\frac{Re}{\alpha}\frac{\partial\omega}{\partial Re}\right)+\left(\frac{z}{t}\right)^2 = 0. \tag{4.2}$$

Thus, for a given set of $(x/t, z/t)$, $\alpha$ can be found from this equation and the saddle-point value for $(a, b)$ can then be obtained from equation (4.1). In doing so, several points need to be cleared up.

First, it can be seen that, when

$$\frac{\partial\omega}{\partial\alpha}-\frac{\omega}{\alpha}-\frac{Re}{\alpha}\frac{\partial\omega}{\partial Re} = 0, \tag{4.3}$$

the equation (4.1) does not yield solutions for $(a, b)$. However, this occurs at most at isolated points in the $\alpha$-plane, because the condition (4.3) implies that

$$\alpha\frac{\partial}{\partial\alpha}\left(\frac{\omega}{\alpha}\right)-Re\frac{\partial}{\partial Re}\left(\frac{\omega}{\alpha}\right) = 0,$$

which is true only if the complex wave speed $c = \omega/\alpha$ is a function of $\alpha Re$ alone. This condition is not generally satisfied by solutions of the Orr–Sommerfeld equation which has coefficients involving both $\alpha^2$ and $\alpha Re$ so that $c$ is usually a function of both. In any case, the existence of such isolated points is irrelevant to the calculation of the saddle points since they do not satisfy the equation (4.2), unless the imaginary parts of both $\partial\omega/\partial\alpha$ and $\omega/\alpha + (Re/\alpha)\,\partial\omega/\partial Re$ are zero.

In our calculations we have not noticed any difficulties due to the condition (4.3), because there are no values of $\alpha$ that satisfy both (4.3) and (4.2) in our problem. However, it is theoretically possible for this to occur and for this reason, we will briefly discuss a way of overcoming such difficulties. If the original saddle-point equations (3.3) are used to calculate $(a, b)$ directly from the three-dimensional eigenfrequency $\tilde{\omega}(a, b)$, there are no such difficulties. Thus it is clear that these singular points occur entirely as a result of using the Squire transformation. From the numerical calculation point of view, the existence of these isolated points will not affect the calculation of the wave packets since the Jacobian determinant (3.5) under the condition (4.3) is in general not equal to zero and so the result (3.4) is still the leading-order contribution in the asymptotic expansion. Thus, since the difficulties are not associated with any physical phenomenon, the values at these points can be obtained by simply interpolating between the values at neighbouring points.

Second, when calculating the saddle point through (4.2), false solutions may be introduced. This is because equation (4.2) is obtained by manipulating (4.1) with its second equation squared. If this occurs, the false solutions can be rejected by examining equation (4.1). This can be clearly demonstrated by considering the special case of $z/t = 0$. In this case, (4.2) yields two saddle points given by

$$\frac{x}{t} - \frac{\partial\omega}{\partial\alpha} = 0, \quad \frac{x}{t} - \frac{\omega}{\alpha} - \frac{Re}{\alpha}\frac{\partial\omega}{\partial Re} = 0.$$

The first is the same as the saddle-point equation for the two-dimensional case (Gaster 1968*b*), while the second one gives a false solution. To show this, we set $z/t$ to zero in equation (4.1). The second equation of (4.1) then seems to permit three solutions

$$\text{(i)} \quad a = 0;$$

$$\text{(ii)} \quad \frac{\partial\omega}{\partial\alpha} - \frac{\omega}{\alpha} - \frac{Re}{\alpha}\frac{\partial\omega}{\partial Re} = 0;$$

$$\text{(iii)} \quad b = 0.$$

The first choice must be ruled out because the Orr–Sommerfeld equation would only have a trivial zero solution. The second choice is not possible because it is exactly the condition (4.3) discussed above which is not on the saddle-point trace for this problem. Thus the only proper solution is the third one, which can also be readily derived by the symmetry of $\tilde{\omega}(a, b)$ in the wavenumber $b$ in both inviscid and viscous cases. This solution actually coincides with the saddle-point trace in the two-dimensional case, because the first equation in the Squire transformation (3.6) gives $a = \alpha$ and the first equation of (4.1) gives $x/t = \partial\omega/\partial\alpha$.

Third, for a given value of $x/t$ and $z/t$, there may be more than one saddle point. If they are inherent for the given problem, they should all be taken into account, with the wave packet given by the summation of terms of the form (3.4) over all the saddle points. In the spirit of asymptotic analysis, only the one of these solutions that gives the largest amplification is needed. However, the multi-valued $\alpha$

determined by (4.2) may be a result of the squaring of the wavenumbers involved in the Squire transformation. If this is the case, the problem of choosing the correct Riemann surface when using (4.2) to find the saddle points is entirely mathematical; it results purely from the use of the Squire transformation and the two-dimensional eigenfrequency $\omega(\alpha, Re)$, regardless of whether the problem is viscous or inviscid. By regarding $\alpha$ as a function of $x/t+\mathrm{i}z/t$, it is clear that the correct Riemann surface must be chosen in the complex plane $x/t+\mathrm{i}z/t$. To do this, we can use the principle of analytic continuation and consider the function $\alpha$, of complex argument $x/t+\mathrm{i}z/t$, to be the analytic continuation from its values on the real axis $x/t = 0$ in the complex $(x/t, z/t)$-plane. Thus, the criterion for choosing the correct $\alpha$ is to ensure that the chosen branch contains the values of $\alpha$ on the axis $z/t = 0$. This corresponds to the two-dimensional problem where $\alpha$ is unambiguously determined by $\mathrm{d}\omega/\mathrm{d}\alpha = x/t$ as a function of $x/t$ (Gaster 1968*b*). This principle must also be used to determine the correct branch for $a$ when it is calculated from (4.1). In fact, as will be shown later on, the wave packet solution, (3.4), can be expressed in terms of $\alpha$ and one of many expressions involving the wavenumber $a$. It is thus sufficient to specify the branch for any one of such expressions.

## 5. Saddle-point analysis for an inviscid wake flow

In this section, we demonstrate the use of the analysis in the previous section by examining the inviscid wake flow with the mean velocity profile given by

$$\bar{U}(y) = 1-0.692\exp(-0.693y^2), \tag{5.1}$$

the same one examined by Gaster & Davey (1968) for the development of three-dimensional wave packets. For inviscid flows, the governing Orr–Sommerfeld equation reduces to the Rayleigh equation, which admits both symmetrical and antisymmetrical eigenmodes for the symmetrical mean velocity profile $\bar{U}(y)$. Among these two eigenmodes, the least damped one is symmetrical (Drazin & Howard 1966). The calculation of the eigenvalue $\omega$ can be found in the literature and will not be repeated here. The asymptotic evaluation of wave packets also requires the derivatives of the eigenvalue $\omega$ which, in principle, can be obtained by differentiating the Rayleigh equation with respect to $\alpha$. This will lead to higher-order differential equations. Thus, it is quite time-consuming to compute the eigenvalues and their derivatives from the basic differential equation even for the two-dimensional inviscid case. It is desirable to be able to approximate the eigenvalue relation by simple analytic expressions, which is feasible because the dispersion equation defines the eigenfrequency as an analytic function of the wavenumber, except at some isolated branch points. This was first suggested by Gaster (1968*b*), and later effected by Gaster & Jordinson (1975), who utilized the power series representation to approximate the eigenvalues in some regions of the wavenumber planes in their studies of the Blasius boundary-layer flow. Gaster (1978) has further demonstrated that the rate of convergence of the series can be improved by resorting to the nonlinear Shanks transformation. An alternative is the adoption of an algebraic model expansion for the complex dispersion relation (Craik 1981, 1982). By suitable choice of parameters, Craik was able to recover the results in different flows.

In this paper the eigenvalue relation is represented by a rational-fraction function obtained by the application of the Padé approximant method (Baker 1975) to the power series representation. Owing to its ability to map away singularities, the Padé approximant method has been widely used in many subjects, but not previously

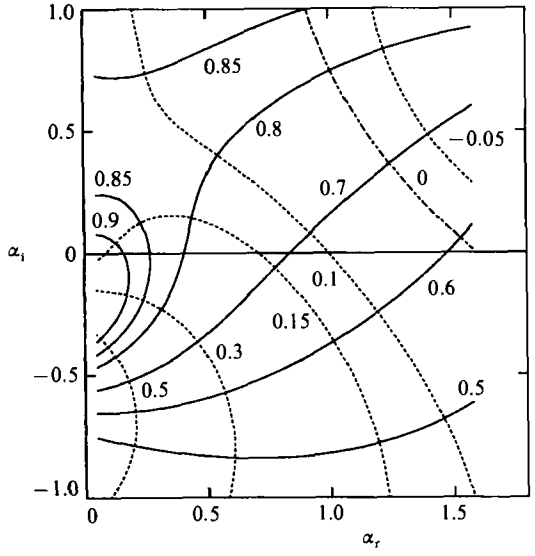


FIGURE 1. Contours of complex wave speed $c = \omega/\alpha$ in the $\alpha$-plane with solid curves representing the real part and broken curves the imaginary part.

in stability studies though it was suggested by Gaster (1978) as an alternative scheme to improve the convergence of the power series representation. Its efficiency and advantages over the techniques being currently used have been discussed by Jiang (1990) for both inviscid and viscous problems. The Padé approximant method replaces the power series representation of the function by a ratio of two polynomials with its numerator $P(\alpha)$ being of degree $L$ and denominator $Q(\alpha)$ of degree $M$, i.e.

$$\omega(\alpha) = P^{[L/M]}(\alpha)/Q^{[L/M]}(\alpha). \tag{5.2}$$

The coefficients of the powers in the numerator and the denominator are calculated by matching the Taylor series expansion of this fraction with the power series. The approximants for $L = M$ are connected to some continued fractions that can improve the convergence properties of a power series remarkably. One of them, $L = M = 7$, will be used in the following numerical calculation.

For inviscid flows, the saddle-point equations (4.1) reduce to

$$\left.\begin{aligned} \frac{x}{t} &= \left(\frac{\mathrm{d}\omega}{\mathrm{d}\alpha} - \frac{\omega}{\alpha}\right)\frac{a^2}{\alpha^2} + \frac{\omega}{\alpha} \\ \frac{z}{t} &= \left(\frac{\mathrm{d}\omega}{\mathrm{d}\alpha} - \frac{\omega}{\alpha}\right)\frac{ab}{\alpha^2} \end{aligned}\right\}. \tag{5.3}$$

Combination of these two equations leads to the inviscid version of (4.2),

$$\left(\frac{x}{t} - \frac{\omega}{\alpha}\right)\left(\frac{x}{t} - \frac{\mathrm{d}\omega}{\mathrm{d}\alpha}\right) + \left(\frac{z}{t}\right)^2 = 0, \tag{5.4}$$

which can be used to calculate $\alpha$ for given values of $(x/t, z/t)$. Then $(a, b)$ can be determined by (5.3), except at some isolated points in the complex $\alpha$-plane where

$$\frac{\mathrm{d}\omega}{\mathrm{d}\alpha} - \frac{\omega}{\alpha} = \alpha \frac{\mathrm{d}}{\mathrm{d}\alpha}\left(\frac{\omega}{\alpha}\right) = 0.$$

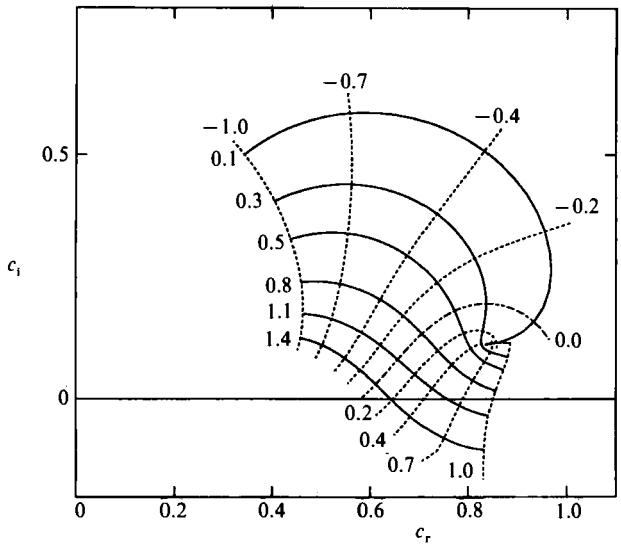


FIGURE 2. Contours of the complex wavenumber $\alpha$ in the wave speed $c = \omega/\alpha$ plane, where the solid curves are the real part and the broken curves the imaginary part.

Singularities occur either at $\alpha = 0$ or when the wave speed $c = \omega/\alpha$ has a vanishing derivative with respect to $\alpha$. The former is a trivial case, while the latter has been observed to occur in inviscid two-dimensional flows (Betchov & Criminale 1966, Mattingly & Criminale 1972, Gaster & Jordinson 1975). To explore the possibility of $\mathrm{d}c/\mathrm{d}\alpha = 0$, contours of $c$ in the complex $\alpha$-plane are plotted in figure 1. It is obvious that there is at least one point where the wave speed has a zero derivative, which occurs at about $\alpha = 0.11202 + \mathrm{i}0.45229$. This can also be demonstrated by plotting contours of $\alpha$ in the complex $c$-plane, as presented in figure 2. There is evidently a branch point singularity in the $c$-plane. This singular behaviour of $\alpha$ as a function of $c$ can be understood by expanding $c(\alpha)$ at the point where $\mathrm{d}c/\mathrm{d}\alpha = 0$. The leading term in the expansion is proportional to the square of $\alpha$; the inverse function $\alpha(c)$ at the corresponding point is then a square root function of $c$. As analysed in the previous section, these singular points do not, in general, coincide with the saddle point, since they do not satisfy the saddle-point equation which requires $(\omega/\alpha)_i = c_i = 0$.

Separating the real and imaginary parts of the saddle-point equation (5.4) and solving the two equations for $x/t$ and $z/t$, one can derive

$$\left.\begin{aligned} \frac{x}{t} &= \left(\frac{\omega}{\alpha}\frac{\mathrm{d}\omega}{\mathrm{d}\alpha}\right)_i \Big/ \left(\frac{\omega}{\alpha}+\frac{\mathrm{d}\omega}{\mathrm{d}\alpha}\right)_i \\ \frac{z}{t} &= \pm\left[\left(\frac{\omega}{\alpha}\right)_i\left(\frac{\mathrm{d}\omega}{\mathrm{d}\alpha}\right)_i\right]^{\frac{1}{2}}\left[1+\left(\frac{\mathrm{d}\omega}{\mathrm{d}\alpha}-\frac{\omega}{\alpha}\right)_r^2 \Big/ \left(\frac{\mathrm{d}\omega}{\mathrm{d}\alpha}+\frac{\omega}{\alpha}\right)_i^2\right]^{\frac{1}{2}} \end{aligned}\right\}. \tag{5.5}$$

These define $x/t$ and $z/t$ as functions of $\alpha$, provided that

$$\left(\frac{\omega}{\alpha}\right)_i\left(\frac{\mathrm{d}\omega}{\mathrm{d}\alpha}\right)_i \geqslant 0, \quad \left(\frac{\omega}{\alpha}+\frac{\mathrm{d}\omega}{\mathrm{d}\alpha}\right)_i \neq 0. \tag{5.6}$$

The curves of $(\omega/\alpha)_i = 0$, $(\mathrm{d}\omega/\mathrm{d}\alpha)_i = 0$ and $(\omega/\alpha + \mathrm{d}\omega/\mathrm{d}\alpha)_i = 0$ in the complex $\alpha$-plane are shown in figure 3. The condition (5.6) is satisfied in the regions to the left

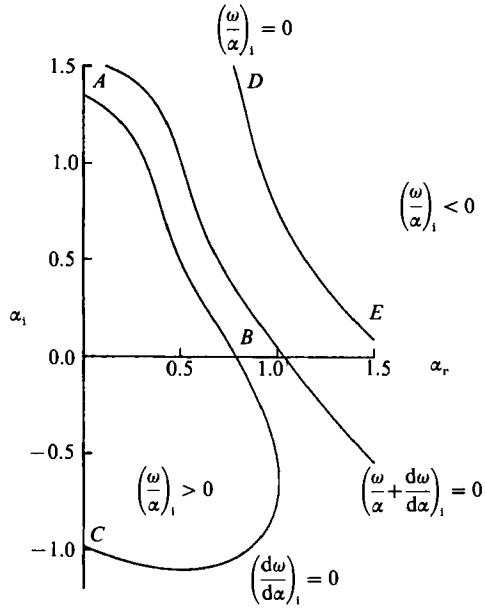


FIGURE 3. The complex $\alpha$-plane where $\omega(\alpha)$ is the eigenfrequency.

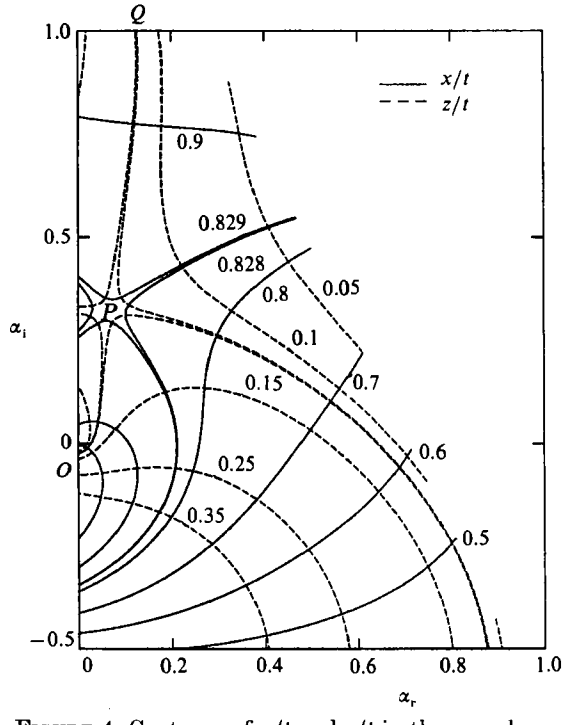


FIGURE 4. Contours of $x/t$ and $z/t$ in the complex $\alpha$-plane.

of the curve $ABC$, and to the right of the curve $DE$. Solutions to the right of $DE$, however, are spurious solutions, introduced when taking squares of (5.3) to combine them into (5.4). As explained in the previous section, this can be seen by comparing the solutions of the original equation (5.3) with those of (5.4). Taking again the case

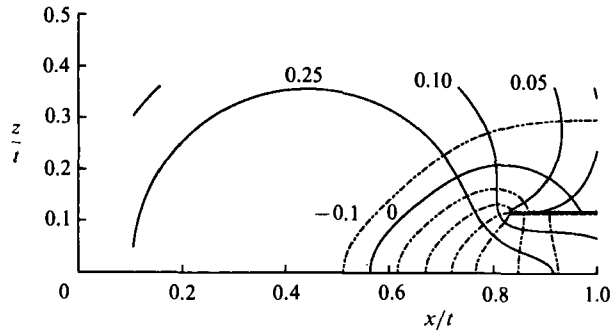


FIGURE 5. Contours of $\alpha_r$ (solid curves) and $\alpha_i$ (broken curves) in the $(x/t, z/t)$-plane.

of $z/t = 0$ as an example, (5.3) gives a unique solution determined by $x/t = \mathrm{d}\omega/\mathrm{d}\alpha$ and $b = 0$ (corresponding to the two-dimensional case). When using (5.4), however, we find two solutions, one on the curve $ABC$ and the other on the curve $DE$. The one on the curve $ABC$ is the same as that given by (5.3), and hence is the correct solution. The solution on $DE$ is a false solution because it does not satisfy (5.3), from which (5.4) is derived.

Therefore, for non-zero values of $z/t$, the saddle points are located in the region to the left of the curve $ABC$. In this region, unique values of $(x/t, z/t)$ can be calculated from (5.5) for given $\alpha$, but the inverse, that is, the evaluation of $\alpha$ for given $(x/t, z/t)$, which is our main concern, is not so straightforward. This is because $\alpha$ is a double-valued function of $x/t + \mathrm{i}z/t$, which is clearly shown in figure 4. The contours of $x/t$ and $z/t$ given by (5.5) are plotted in the complex $\alpha$-plane in this figure, which shows that at the point marked $P$, the gradient of the quantity $x/t + \mathrm{i}z/t$ as a function of $\alpha$ vanishes, so that it can be written as

$$x/t + \mathrm{i}z/t \sim (x/t)_\mathrm{p} + \mathrm{i}(z/t)_\mathrm{p} + k(\alpha - \alpha_\mathrm{p})^2 \quad \text{as } \alpha \to \alpha_\mathrm{p}, \tag{5.7}$$

where $(x/t)_\mathrm{p}$ and $(z/t)_\mathrm{p}$ are values of $(x/t, z/t)$ at $\alpha = \alpha_\mathrm{p}$ (see also figure 5),

$$(x/t)_\mathrm{p} \approx 0.82862, \quad (z/t)_\mathrm{p} \approx \pm 0.11570.$$

Since the leading-order term involving $\alpha$ in (5.7) is a square, the inverse function must have a square root branch point at $(x/t)_\mathrm{p} + \mathrm{i}(z/t)_\mathrm{p}$. Thus, a branch cut must be determined in the complex $(x/t, z/t)$-plane and the correct Riemann surface needs to be chosen for $\alpha$.

As discussed in the previous section, this branch cut is actually set by the requirement that the chosen branch of $\alpha$ for non-zero $z/t$ must contain its values for $z/t = 0$, that is, by the principle of analytic continuation that the values of $\alpha$ for the three-dimensional problem must be in the same Riemann surface as those for the two-dimensional one. The saddle-point trace for the case $z/t = 0$ is on the curve $ABC$ in figure 3, which is on the right-hand side of the curve $OPQ$ in figure 4. The curve $OPQ$ divides the complex $\alpha$-plane into two. The region to the right contains the corresponding two-dimensional case (a segment of the curve $ABC$), and hence is the correct analytic continuation. Thus only this region is physically relevant and maps to the whole complex $(x/t, z/t)$-plane, which is shown in figure 5. The branch cut in the $(x/t, z/t)$-plane is, as a result, given by a horizontal line parallel to the $(x/t)$-axis from the point $(x/t)_\mathrm{p} + \mathrm{i}(z/t)_\mathrm{p}$ to infinity, as displayed, and corresponds to the curve $PQ$ (or $PO$) in figure 4.

## 6. Three-dimensional wave packets

Having determined the correct branch for $\alpha$, its values can be found from the saddle-point equation (5.4). The corresponding values of $(a, b)$ can then be derived from (5.3), which once again requires the specification of the correct branch because $a^2$ is involved in these equations. In fact, it is sufficient to specify the branch for any expression involving $a$ because the asymptotic solution (3.4) can be expressed in terms of $\alpha$ and one of such expressions. In the inviscid case, the wave-packet solution assumes the form

$$\hat{v}(x, y, z, t) = \frac{-g(a, \alpha, y)}{2\pi t[-J(\alpha)]^{\frac{1}{2}}} e^{\psi t}, \tag{6.1}$$

where $g$ is the function of $a$, $\alpha$, $y$ instead of $a$, $b$, $y$ now, the Jacobian determinant $J$ is entirely given by $\alpha$ as

$$J = -\frac{1}{\alpha}\left(\frac{x}{t}-\frac{\omega}{\alpha}\right)\frac{d^2\omega}{d\alpha^2}+\frac{1}{\alpha^2}\left(\frac{x}{t}-\frac{d\omega}{d\alpha}\right)\left(\frac{d\omega}{d\alpha}-\frac{\omega}{\alpha}\right), \tag{6.2}$$

and the complex phase function $\psi$ can be written as

$$\psi = i\alpha\left(\frac{d\omega}{d\alpha}-\frac{\omega}{\alpha}\right), \tag{6.3}$$

$$= i\alpha\left[\left(\frac{x}{t}-\frac{\omega}{\alpha}\right)^2+\left(\frac{z}{t}\right)^2\right]^{\frac{1}{2}}. \tag{6.4}$$

Here the last step follows from the use of (5.4) and the first equation in (5.3), which gives $a$ as

$$a = \alpha\left[\frac{x/t-\omega/\alpha}{d\omega/d\alpha-\omega/\alpha}\right]^{\frac{1}{2}}. \tag{6.5}$$

To determine $\psi$ we can specify either the square root in (6.4) or that in (6.5). In both cases, the criterion is the same as that in choosing $\alpha$, namely, to regard the functions as their analytic continuation from the two-dimensional case. If we choose to work with (6.5), the square root is chosen to ensure that $a \to \alpha$ when $z/t \to 0$ since when $z/t = 0$, $x/t = d\omega/d\alpha$ and

$$\frac{x/t-\omega/\alpha}{d\omega/d\alpha-\omega/\alpha} = 1.$$

Thus, we can choose the branch such that the real part of the square root in (6.5) is positive, namely, $(a/\alpha)_r > 0$. This is in fact the condition noticed by Gaster & Davey (1968), and corresponds to growing oblique waves. Alternatively, if we work on (6.4), the square root in it reduces, in the limit $z/t \to 0$, to $x/t-\omega/\alpha$, which has positive imaginary parts $(\omega/\alpha)_i$ in the two-dimensional limit. The branch can be chosen according to this, which leads to the condition $(\psi/\alpha)_r < 0$.

Having determined the branches, the velocity perturbation $\hat{v}(x, y, z, t)$ is now uniquely determined by (6.1) for given $(x/t, z/t)$. The instability characteristics of this result can be examined through its amplification contours, namely, the contours of the real part of the complex phase function $\psi$, which we plot in the complex $(x/t+iz/t)$-plane in figure 6. The solid curves in this figure denote positive real parts

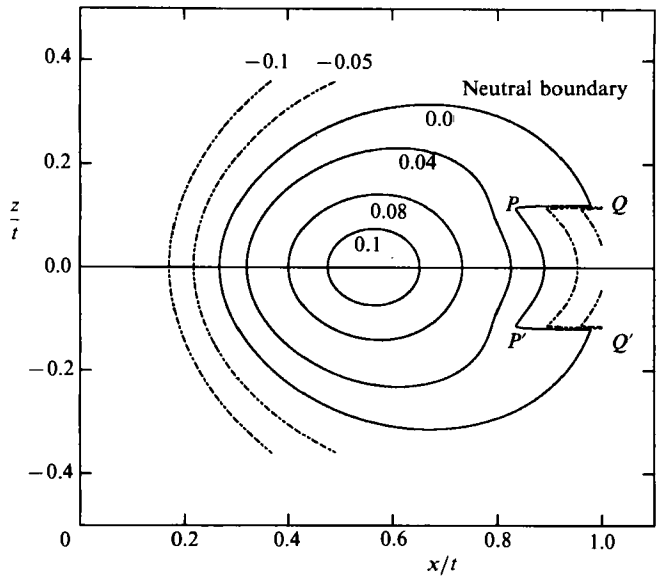


FIGURE 6. Contours of the real part of the phase function $\psi$ in the $(x/t, z/t)$-plane.

of $\psi$, and hence correspond to amplifying waves. The waves occupy a region that is almost elliptic except for a concave front edge. Most of the contours in this figure are in agreement with those derived by Gaster & Davey (1968) (see their figure 3). Although they did require $(a/\alpha)_r > 0$, corresponding to positive real parts of the square root in (6.5), in order to obtain the amplified oblique waves, they mistook the curve of $a_r = 0$ for the curve of $(a/\alpha)_r = 0$ and did not choose the correct Riemann surface for $\alpha$. Owing to this mistake they found a discontinuity at the front edge of the wave packet. Thus they did not give a complete amplification contour and did not describe the wave packet. They conjectured that this discontinuity might be caused by the assumption of the inviscid flow and that viscosity might smooth it out. If this were the case, the wave packet would have a large velocity gradient near the forward edge which would still cause breakdown into turbulence to occur in this region first. From the analysis given here, it is clear that this discontinuity is caused by their choice of the branch cuts; when the cuts are correctly chosen, the discontinuity is no longer there. Comparing figure 6 here with their figure 3, it can be seen that the region enclosed by *BODB* in their figure 3 is a damped region, as they predicted. However, for the region in the vicinity of the point $Q$, they chose values of $\alpha$ on the left-hand side of the curve *OPQ* in figure 4 as the saddle points, causing the discontinuity in this region.

To evaluate the result (6.1), it is necessary that the Jacobian determinant (6.2) does not vanish. In the region of interest here, this vanishing occurs only at the branch point $P$, that is, at $(x/t)_p \approx 0.82862$ and $(z/t)_p \approx \pm 0.11570$. To demonstrate this, the curves of vanishing real and imaginary part are plotted in figure 7; at their crossing point, the Jacobian determinant equals zero. This crossing point can be identified to be the point $P$, because at that point $\mathrm{d}(x/t)/\mathrm{d}\alpha = 0$ and $\mathrm{d}(z/t)/\mathrm{d}\alpha = 0$; and substituting into the derivative of (5.4) immediately shows the Jacobian determinant to be zero. Thus at this branch point, the expansion (6.1) is no longer the leading-order term and the Airy integral should be used to give the proper asymptotic expansion. However, it is reasonably to expect that the error will not be very

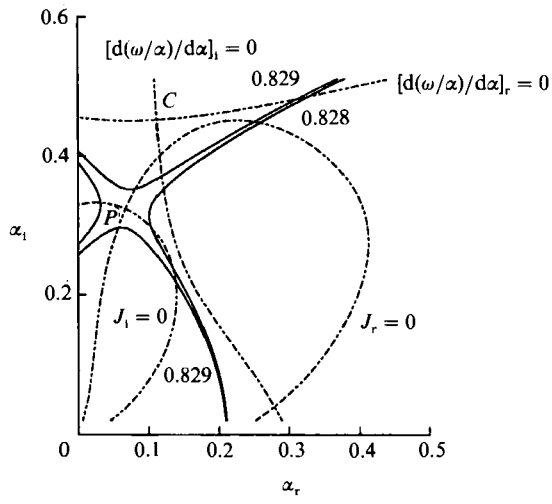


FIGURE 7. The complex $\alpha$-plane where the solid curves are contours of $x/t$.

significant if (6.1) is used in the neighbourhood of the point $P$, and the value at $P$ is then interpolated from these neighbouring points. This is because the point $P$ is on the neutral curve; and the error introduced by interpolating is of algebraic order, which is negligible in comparison with the exponentially growing terms in the region inside the neutral curve. It is plausible to conjecture that similar points will also occur in viscous problems, since (4.1) and (5.3) are very similar in form. The point in figure 7 where $d(\omega/\alpha)/d\alpha = 0$ is marked by $C$ and it can be seen that the Jacobian determinant there is not equal to zero, as predicted for the full viscous problem in §4.

Collecting all the analyses, we can evaluate the characteristic wave packets, given by

$$I_3(x,z,t) = \frac{\hat{v}(x,y,z,t)}{g(a,\alpha,y)} = \frac{-e^{\psi t}}{2\pi t[-J(\alpha)]^{\frac{1}{2}}}. \tag{6.6}$$

Figures 8 and 9 show wave packets at dimensionless times $t = 60$, 80 and 100, in perspective views from both the downstream and the upstream directions. The height of the waves is normalized by the maximum of the wave packet at each different time, in order to show clearly the shape of wave packets. As time increases, the original point disturbance develops into a wavetrain which lasts many wave periods and whose amplitude grows.

To check whether the three-dimensional wave packets have been calculated correctly, one of them at $t = 60$ is integrated over $z$ and the result is then compared with a two-dimensional wave packet for the same time parameter $t = 60$. The two should be equal because

$$\begin{aligned}\int_z \hat{v}(x,y,z,t)\,dz &= \int_z \frac{i}{(2\pi)^2}\int_a\int_b v(y,a,b,\tilde{\omega})\exp[i(ax+bz-\tilde{\omega}t)]\,db\,da\,dz \\ &= \hat{v}_2(x,y,t),\end{aligned}$$

where the subscript 2 is used to denote the velocity for the two-dimensional case. The last step follows from trivially performing the $z$ integral with the result $2\pi\delta(b)$ which is then used to carry out the $b$ integral. This simply means that a point source in the two-dimensional flow is a line source in the three-dimensional flow. The linearity of the governing equations allows a line source to be decomposed into an infinite

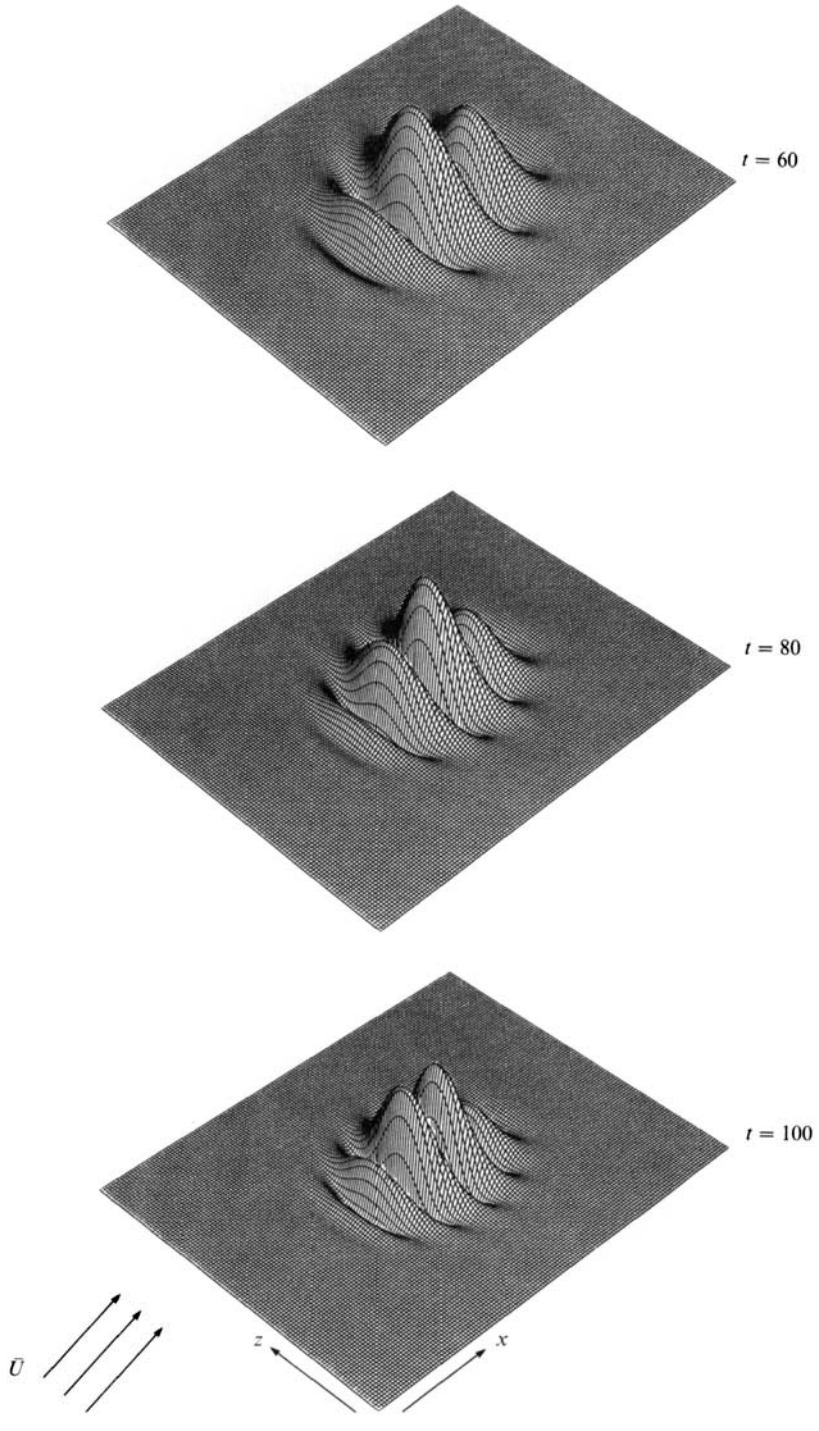


FIGURE 8. A perspective view of the three dimensional characteristic wave packet calculated from (6.6) at time $t = 60$, 80 and 100, viewed from behind the waves.

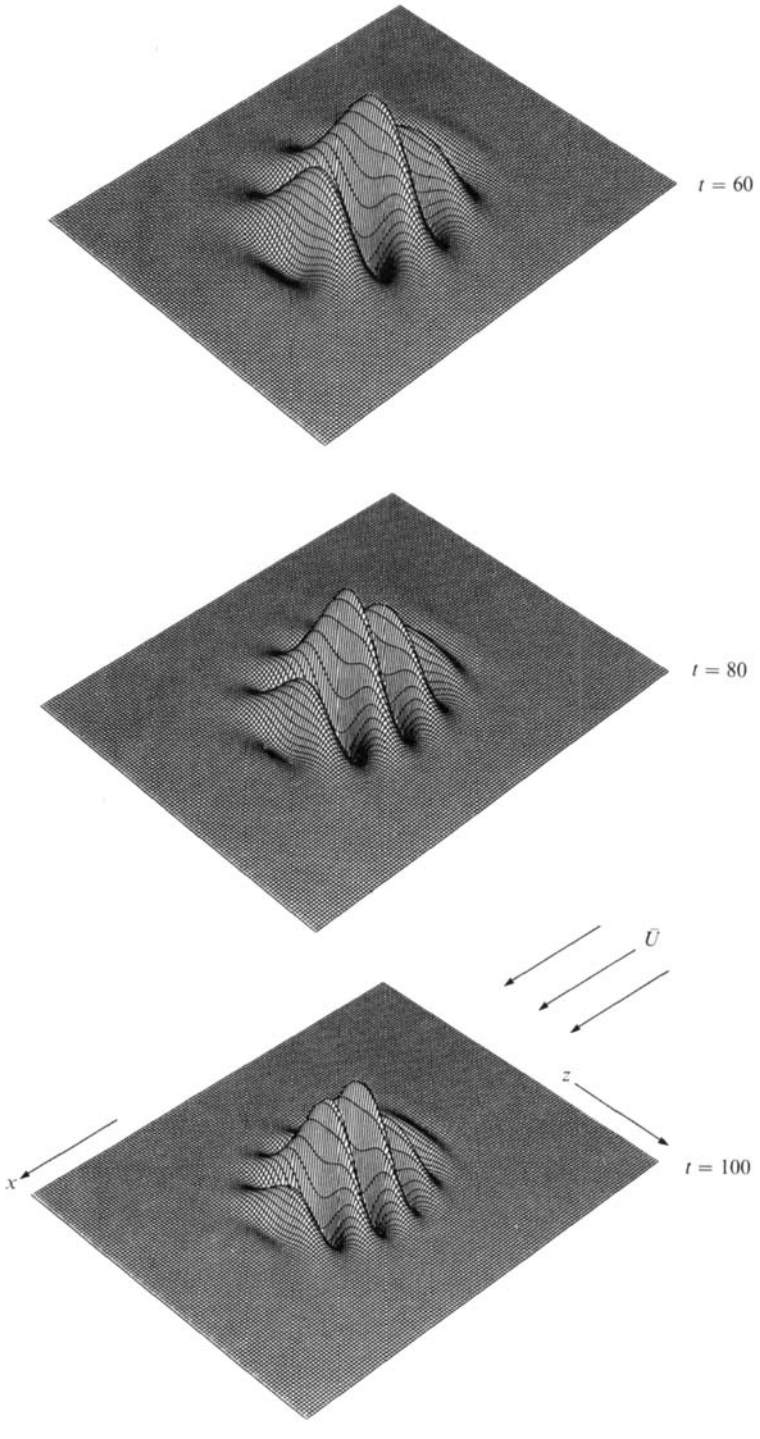


FIGURE 9. The same wave packet as in figure 8, viewed from ahead of waves.

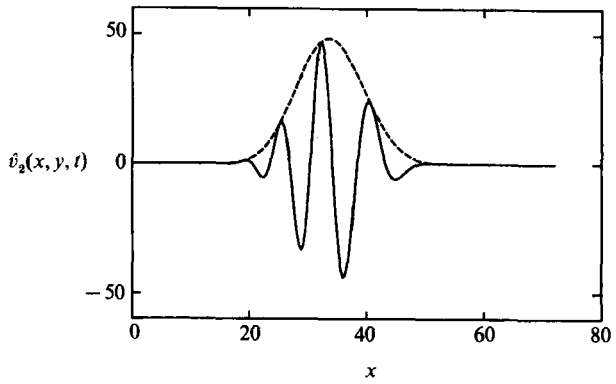


FIGURE 10. Two-dimensional wave packet at $t = 60$, the dashed curve being its envelope.

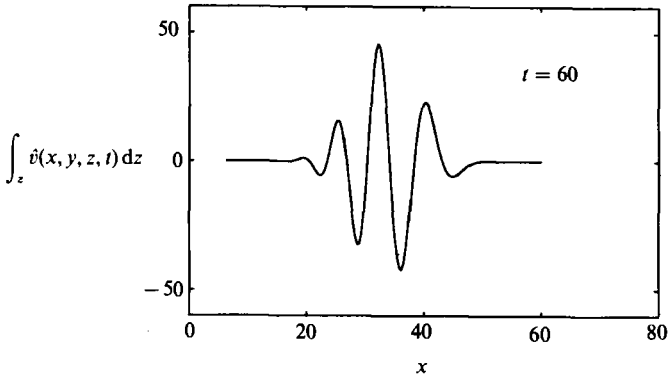


FIGURE 11. The summation of the three-dimensional wave packet over the $z$-direction.

number of point sources. The result of this comparison is shown in figures 10 and figure 11, and the obvious similarity between the two demonstrates the accuracy of the three-dimensional calculations.

## 7. Conclusions

We have evaluated the three-dimensional disturbance waves by the method of steepest descent. In doing so, some difficulties associated with the use of the Squire transformation have been discussed. This transformation reduces the original equations for the saddle point, namely, the vanishing of the gradient of the complex phase function $\psi(a, b)$, to a single equation that links the physical space to the two-dimensional wavenumber $\alpha$. However, this equation defines the saddle-point value of $\alpha$ as a double-valued function of the complex argument $x/t + \mathrm{i}z/t$. There are two sources for this non-uniqueness of solutions; the equation is derived by a manipulation involving squaring operations and the Squire transformation itself contains square-root functions. The spurious solutions introduced by the squaring operation can be rejected by substituting them into the original equations, but the solution due to the inherent square-root functions in the Squire transformation needs much more careful analysis. The correct branch of this multi-valued function for the saddle point can only be selected by resorting to the principle of analytic continuation. This is also the basis for the use of the steepest descent method; it is

based on the assumption that the integrand of the wavenumber inversions in (3.1) can be analytically continued from its original domain of definition, that is, the real axes, to the complex wavenumber planes. Applying this principle and considering the three-dimensional problem as the analytic continuation of the two-dimensional case, the correct Riemann surfaces and branch cuts can be determined. For the wake flow examined by Gaster & Davey (1968), we have pointed out the mistake that they made, which resulted in the discontinuity in their amplification contours and led to some incorrect conclusions. When the proper choices are made the discontinuity disappears and the wave packets can be evaluated. The wave packets have a concave forward edge in the mean flow direction. The calculation of the wave packets was performed with the aid of the Padé approximant method discussed by Jiang (1990).

The author wishes to thank her supervisor Professor M. Gaster, FRS for his continuous guidance and encouragement. She is also grateful to Professor A. D. D. Craik for helpful discussions and comments on an early draft of this paper.

## REFERENCES

BAKER, G. A. 1975 *Essentials of Padé Approximation*. Academic.

BENJAMIN, T. B. 1961 The development of three-dimensional disturbances in an unstable film of liquid flowing down an inclined plane. *J. Fluid Mech.* **10**, 401–409.

BETCHOV, R. & CRIMINALE, W. O. 1966 Spatial instability of the inviscid jet and wake. *Phys. Fluids.* **9**, 359–362.

BETCHOV, R. & CRIMINALE, W. O. 1967 *Stability of Parallel Flows*. Academic.

BETCHOV, R. & SZEWCZYK, A. 1963 Stability of a shear layer between parallel streams. *Phys. Fluids* **6**, 1391–1396.

CRAIK, A. D. D. 1981 The development of wavepacket in unstable flows. *Proc. R. Soc. Lond.* A **373**, 457–476.

CRAIK, A. D. D. 1982 The growth of localized disturbances in unstable flows. *Trans. ASME* E: *J. Appl. Mech.* **49**, 284–290.

CRIMINALE, W. O. & KOVASZNAY, L. S. G. 1962 The growth of localized disturbances in a laminar boundary layer. *J. Fluid Mech.* **14**, 59–80.

DRAZIN, P. G. & HOWARD, L. H. 1966 Hydrodynamic stability of parallel flow of inviscid fluid. In *Advances in Applied Mechanics*, vol. 9 (ed. G. Kuerti), pp. 1–89. Academic.

DRAZIN, P. G. & REID, W. H. 1981 *Hydrodynamic Stability*. Cambridge University Press.

GASTER, M. 1968*a* The development of three-dimensional wave packets in a boundary layer. *J. Fluid Mech.* **32**, 173–184.

GASTER, M. 1968*b* Growth of disturbances in both space and time. *Phy. Fluids* **11**, 723–727.

GASTER, M. 1978 Series representation of the eigenvalues of the Orr–Sommerfeld equation. *J. Comp. Phys.* **29**, 147–162.

GASTER, M. & DAVEY, A. 1968 The development of three-dimensional wave packets in unbounded parallel flows. *J. Fluid Mech.* **32**, 801–808.

GASTER, M. & GRANT, I. 1975 An experimental investigation of the formation and development of a wave packet in a laminar boundary layer. *Proc. R. Soc. Lond.* A **347**, 253–269.

GASTER, M. & JORDINSON, R. 1975 On the eigenvalues of the Orr–Sommerfeld equation. *J. Fluid Mech.* **72**, 121–133.

JIANG, F. 1990 The development of linear wave packets in unbounded shear flows. Ph.D. thesis, Cambridge University Engineering Department.

LIN, C. C. 1955 *The Theory of Hydrodynamic Stability*. Cambridge University Press.

MATTINGLY, G. E. & CRIMINALE, W. O. 1972 The stability of an incompressible two-dimensional wake. *J. Fluid Mech.* **51**, 233–272.